



## Research paper

# Influence of soft layer thickness on the aggregate displacement in the backfill material of dynamic replacement columns – results of laboratory model tests

Sławomir Kwiecień<sup>1</sup>, Siergey Ihnatov<sup>2</sup>, Magdalena Kowalska<sup>3</sup>

**Abstract:** The dynamic replacement columns are formed by driving a coarse-grained material into a soft soil by means of repeatable drops of a pounder. The final shapes of the columns are non-cylindrical and depend on the subsoil conditions. This paper presents results of the laboratory study on influence of the thickness of the soft soil on the displacements of the backfill aggregate during the driving process. A test box with one acrylic-glass wall was prepared, in which, over a load-bearing sand layer, a soft soil of various thicknesses ( $H_s = 0.3, 0.4$  or  $0.5$  m) was modelled using a semi-transparent acrylic polymer. The displacements of the backfill gravel particles were tracked by means of a high-speed camera. The material was driven by dropping a  $0.2$  m high ( $H_p$ ) pounder. The results revealed that the distance between the bottom of the first crater and the top of the sand layer played an important role in directing the particles. At  $H_s/H_p = 2.5$  pear-shaped floating columns were formed as the grains in the side zones were less affected by the pounder drops and their paths deviated from the vertical axis by not more than  $50^\circ$ . In case of  $H_s/H_p = 2.0$  and  $1.5$ , the column bases reached the bearing layer and the impact energy caused much larger vertical and horizontal displacements of the backfill material in the side zones – the observed largest angles were equal to  $64^\circ$  and even  $90^\circ$ , respectively. Eventually, the final column shapes resembled a non-symmetrical barrel and a truncated cone.

**Keywords:** aggregate displacement paths, dynamic replacement, geotechnical engineering, ground improvement, stone columns, soft soil

<sup>1</sup>DSc., PhD., Eng., Silesian University of Technology, Faculty of Civil Engineering, ul. Akademicka 5, 44-100 Gliwice, Poland, e-mail: [slawomir.kwiecien@polsl.pl](mailto:slawomir.kwiecien@polsl.pl), ORCID: 0000-0001-6401-2471

<sup>2</sup>PhD., Eng., Silesian University of Technology, Faculty of Civil Engineering, ul. Akademicka 5, 44-100 Gliwice, Poland, e-mail: [siergey.ihnatov@polsl.pl](mailto:siergey.ihnatov@polsl.pl), ORCID: 0000-0002-5747-291X

<sup>3</sup>PhD., Eng., Silesian University of Technology, Faculty of Civil Engineering, ul. Akademicka 5, 44-100 Gliwice, Poland, e-mail: [magdalena.kowalska@polsl.pl](mailto:magdalena.kowalska@polsl.pl), ORCID: 0000-0001-7549-2722

## 1. Introduction

Dynamic replacement (DR) is one of the deep-ground improvement methods, that has been used worldwide for almost 50 years [1, 2]. This procedure involves the formation of columns in the ground by dropping a large mass pounder (3.6–26 tonnes [3, 4]) from the height of 15–25 m [1] and filling the obtained crater with a coarse material. Sandy, gravelly and, most frequently, cobbly fractions are used here. The pounder drops and the void backfilling is repeated several times. As the material is forced into the ground, it travels downwards and sideways, eventually creating a non-cylindrical column, whose diameter varies with the depth [4]. The maximum final length of a typical end-bearing column is usually 5–7 m [4, 6, 7]. The *in situ* measurements of the as-built columns, conducted by one of the authors [5, 8, 9], proved that the ground conditions have a great influence on the final shape of the columns. One of the most important factors is the ratio of the soft soil layer thickness and the height of the pounder.

This observation has prompted the authors to undertake a medium-scale laboratory research on the process of the aggregate displacement during forming of DR columns in soft layers of different thicknesses. The starting points of the study were: (a) the construction of a special testing stand enabling the observation of the column formation process and (b) selection of a material that could simulate a very soft soil layer and was highly transparent. The first requirement was met by building a cuboid box with an acrylic-glass front wall. The second one – by choosing a crosslinked hydrophilic water-soluble acrylic polymer [10], which after mixing with water was taking the form of a very soft gel (hydrogel).

## 2. Shapes of the dr columns *in situ*

The shapes of the columns formed by the dynamic replacement technique in the field conditions have been studied by one of the authors since 2007. The total of 65 end-bearing and floating columns were investigated [5, 8, 11]. It has been noticed that certain relationships exist between the shapes of the end-bearing columns and the ratio of the thickness of the soft soil layer ( $H_s$ ) to the height of the used pounder ( $H_p$ ) [9]. When the soft soil thickness was about 1.4 times larger than  $H_p$ , the columns took a shape of a truncated cone with the largest diameter at the base (Fig. 1a). The columns formed in the soft soil as thick as  $1.6$ – $2.1H_p$  had a symmetrical or asymmetrical barrel shape – their largest diameters occurred between 50% (Fig. 1c) and 70% (Fig. 1b) of the column length (measured from the terrain surface), which corresponded to the depth of the softest layer. On the other hand, in the case of the floating columns, executed in the grounds with very thick layers of soft soils ( $H_s/H_p > 2.1$ ), the most frequently observed was the shape of a pear – see Fig. 1d [5].

The above results were taken into account while selecting the thicknesses of the soft layers for the laboratory tests.

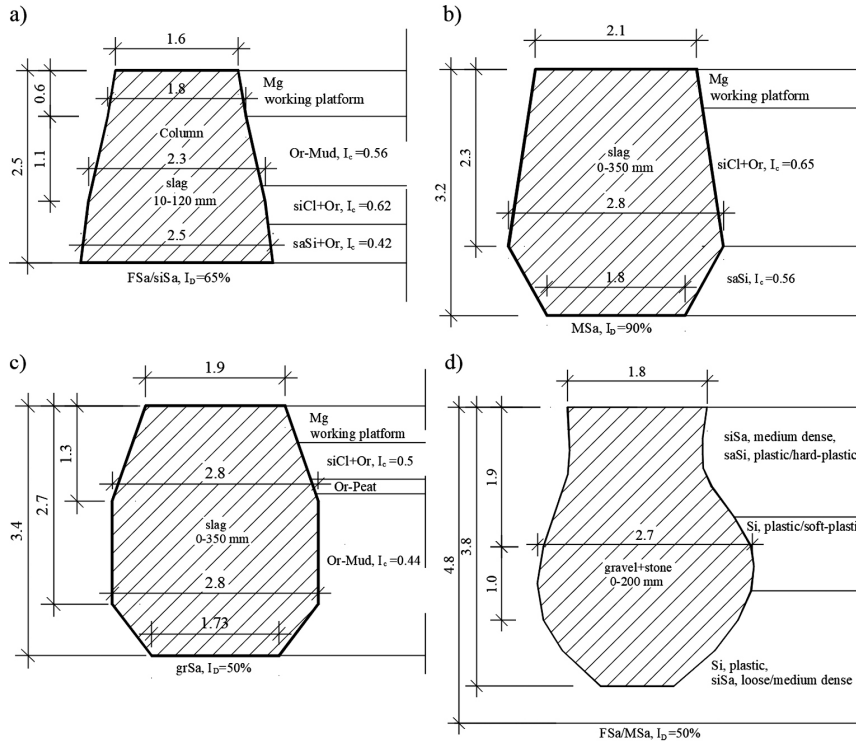


Fig. 1. The shapes of the DR columns at variable thickness of the soft soil layer: a)  $H_s/H_p = 1.4$  [9], b)  $H_s/H_p = 1.8$  [9], c)  $H_s/H_p = 1.9$  [9], d)  $H_s/H_p = 2.7$  [5] (dimensions in meters)

### 3. Testing stand and used materials

The testing stand was prepared in such a way that it was possible to observe the complete process of the dynamic replacement. The experiments were carried out in a cuboid test box with the external dimensions of 1.5 m (width)  $\times$  1.0 m (height)  $\times$  0.15 m (thickness) and an acrylic-glass pane as the front wall (Fig. 2a). The thickness of the wooden walls of the box was 18 mm and the thickness of the acrylic glass was 16 mm.

The dimensions of the poulder, the grain size distribution of the aggregate used in the columns and the thickness of the soft soil were selected using the 1:10 ratio in relation to the average real conditions.

The columns were formed by means of the barrel-like poulder (Fig. 2b) of mass 11.02 kg, similar in shape to the one that is the most commonly used in practice. Its height was equal to 200 mm, the thickness: 120 mm, the width at the centre: 105 mm and at the top and bottom: 90 mm. The poulder was dropped in a guiding square tube resting on the top of the box (Fig. 3), which facilitated the repeated drops from the fixed heights (0.2–1.4 m).

The process of the DR columns' forming was recorded with the use of a 50 fps (frames per second) camera mounted on a tripod. A photographic documentation was also made

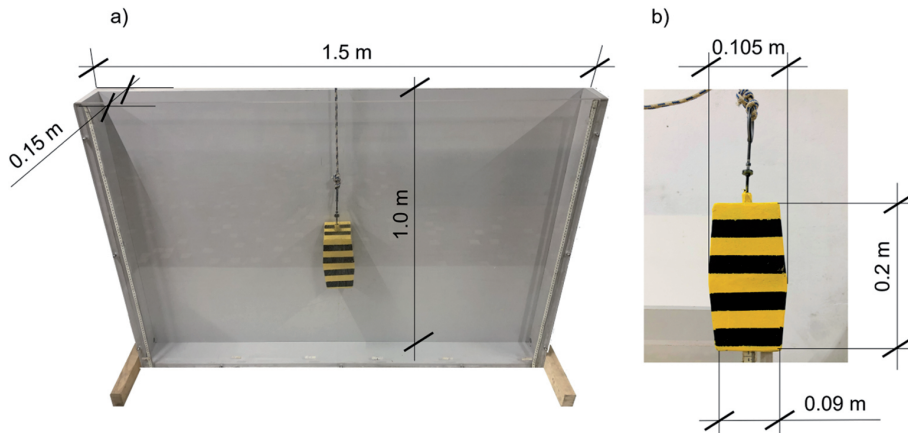


Fig. 2. The test box (a) and the pounder (b), [photo: S. Kwiecień]

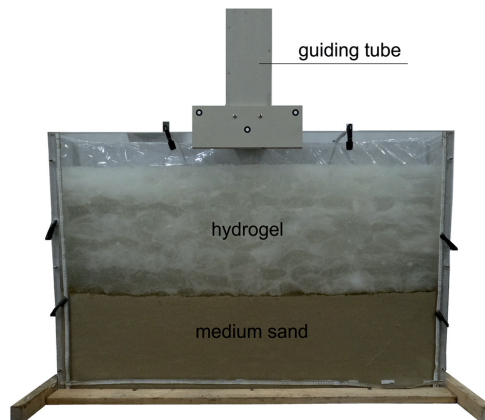


Fig. 3. The test box with the guiding tube, prepared for execution of the column A ( $H_s/H_p = 2.5$ )

for each stage of the study. The software GOM [12] was used to analyse the paths of the backfill material grains in the soft hydrogel layer. The absolute displacement vectors of the driven particles were determined at each pounder drop and the final shape of the column was described. The photos saved in GOM were pasted to the Autocad and the displacement paths were carefully analysed. The lengths and inclinations of the extreme paths (the longest/shortest and the least/most inclined) were recorded.

In the ground improvement with the use of the DR technique, three material zones can usually be distinguished: the soft soil(s), the underlying hard soil layer with relatively high shear strength and stiffness, and the dynamic replacement columns. In the experiments, these zones were simulated with the use of three different materials. The bearing layer, 0.4 m thick, was built of medium sand (MSa). The columns were made of medium gravel (MGr).

The soft layer was modelled with the acrylic polymer (p) mixed with the room-temperature distilled water (w) in the ratio  $p/w = 1:15$  (by weight). The mixture was semi-transparent and in a very soft consistency. Its density was equal to  $1.00 \text{ t/m}^3$ . The amount of water to be added had been determined in a series of empirical experiments, in which the material transparency and state were analysed. When the  $p/w$  ratio was greater than  $1:15$ , it was very difficult to mix the polymer with water as it reacted too fast and formed white inclusions that did not dissolve even if long and intensive mixing was applied. On the other hand, at the  $p/w$  ratio smaller than  $1:15$  the hydrogel was liquid.

Before commencing the main tests, the physical and mechanical properties of the sand and gravel were determined. They included the grain size distribution by means of the sieve analysis method (PN-EN ISO 17892-4 [13]) with determination of the average particle diameter  $d_{50}$ , coefficient of uniformity  $C_U$  and coefficient of curvature  $C_C$ ; the minimum and maximum dry densities ( $\rho_{d.\text{min}}$  and  $\rho_{d.\text{max}}$ ) (PN-88/B-04481 [14]); the specific density  $\rho_s$  (PN-EN ISO 17892-3 [15]), the internal angle of friction  $\varphi$  and cohesion  $c$  in the direct shear tests (PN-EN ISO 17892-10 [16]) and primary and secondary constrained compression moduli in oedometer tests ( $M_0$  and  $M$ ) (PN-EN ISO 17892-5 [17]). The obtained values of the parameters are presented in Table 1 and Table 2.

Table 1. Selected physical properties of the used soils

#	Type of soil	$d_{50}$ [mm]	$C_U$ [-]	$C_C$ [-]	$\rho_s$ [t/m <sup>3</sup> ]	$\rho_{d.\text{min}}$ [t/m <sup>3</sup> ]	$\rho_{d.\text{max}}$ [t/m <sup>3</sup> ]
1.	MSa	0.30	3.33	0.92	2.68	1.59	1.94
2.	MGr	9.70	3.43	1.59	2.66	1.50	1.83

Table 2. Selected mechanical properties of the used soils

#	Type of soil	$\rho_d$ [t/m <sup>3</sup> ]	$\varphi$ [°]	$c$ [kPa]	$M_0$ [MPa]*,**	$M$ [MPa]**
1.	MSa	1.59	29.9	2.61	4.1–38.0	14.5–93.5
2.	MSa	1.80	33.6	4.65	8.3–74.9	38.0–108.5
3.	MGr	1.53	36.1	22.6	6.2–44.8	93.3–124.1
4.	MGr	1.82	42.5	49.6	19.6–102.9	100.4–192.9

\*For comparison with  $M$  – the  $M_0$  values are given for the stress range 25–800 kPa

\*\*The first value represents the range 25–50 kPa, the second one: 400–800 kPa

The shear strength parameters of the medium sand were estimated in the classical shear box  $100 \text{ mm} \times 100 \text{ mm}$  in width, while in case of the gravel, the large-scale apparatus was used with the box width of 241 mm. The heights of the specimens were 32.5 mm and 137.8 mm, respectively. The specimens were sheared dry with the velocity of 1 mm/min. The applied vertical stresses were equal to ca. 50, 100, 150 and 200 kPa in the case of MSa and 100, 200, 300 and 400 kPa in the case of MGr.

The oedometer tests were conducted at the vertical stresses 25–1200 kPa, where each next one was doubling the previous one. One reloading stage was executed at the vertical stresses: 25–800 kPa. The diameter and height of the MSa specimens were equal to 51.3 mm and 22.6 mm, respectively. The compressibility of the MGr was tested in the large-scale direct shear box and the width of the specimens was equal to 241 mm and the height – 144.5 mm.

The peak shear strength parameters and the constrained stiffness of the sand and gravel, shown in Table 2, were determined at the dry densities close to the lowest and the largest values. The relatively large values of apparent cohesion in gravel result from the dilatancy of grains and their interlocking in the direct shear box [18].

## 4. Research program

The purpose of the research was to establish the influence of the soft soil thickness on the process of the material replacement, so the thickness of the hydrogel layer  $H_s$  was varied in the experiments – it was equal to 0.3, 0.4 or 0.5 m. The  $H_s/H_p$  ratios in the model tests were thus equal to 1.5, 2.0 or 2.5, respectively – which is within the ranges of  $H_s/H_p$  registered in the field studies, discussed in Section 2.

The first material placed in the box was the medium sand. It was compacted in four layers by means of a tamper, obtaining eventually the 0.4 m thick bearing layer with the density index  $I_D$  of about 0.44. Next, the hydrogel was carefully added until a 0.5 m thick layer was formed. Its average density was equal to ca.  $1 \text{ t/m}^3$ . The box was then secured with a plastic foil to protect it from the moisture loss and left for 14 days during which the transparency of the gel increased to the required minimum.

Three series of the tests (1, 2, 3) were conducted and in each of them three columns (A, B, C) were formed. The series 1 started with forming of a gravelly column (A) in 0.5 m thick hydrogel layer. After it was done, the gravel was removed, the hydrogel was evenly mixed and its thickness was decreased to 0.4 m. In these conditions the column B was formed. The procedure was repeated for 0.3 m thick hydrogel layer and the column C. In the next step, the box was emptied, cleaned and prepared for the next round. The experiment was repeated twice (series 2 and 3), so eventually 9 columns were formed in the three different depths of the soft material. The view of the testing stand prepared for the execution of the first DR column is visible in Fig. 3.

The energy of compaction was kept constant in all the tests. The poulder was first dropped from the height of 0.2 m to create the initial crater in the hydrogel layer. In all the analysed cases, its depth was equal to about 0.2 m (initial poulder drive  $S_{p0} = 0.2 \text{ m}$ ). The crater was backfilled with medium gravel to the initial ‘surface’ level. Next, the following sequence of the drop heights was applied: 0.3 m, 0.4 m, 0.5 m, 0.6 m, 0.8 m, 1.0 m, 1.2 m,  $7 \times 1.4 \text{ m}$ , 1.0 m and 0.6 m. After each drop of the poulder the crater was backfilled. In total, the poulder was dropped 16 times on the backfill material – its drives  $S_{pi}$  were recorded and totaled  $\sum S_{pi} (i = 1 \div 16)$ .

The summary of the research program has been shown in Table 3.

Table 3. Summary of the research program

#	Type of column [-]	$H_s$ [m]	$H_s/H_p$	Sequence and heights of the poulder drops	No. of series
1	Column A	0.5	2.5	1 × 0.2 m, 1 × 0.3 m, 1 × 0.4 m, 1 × 0.5 m, 1 × 0.6 m, 1 × 0.8 m, 1 × 1.0 m, 1 × 1.2 m, 7 × 1.4 m, 1 × 1.0 m, 1 × 0.6 m	3
2	Column B	0.4	2.0		3
3	Column C	0.3	1.5		3

## 5. Results

The results of the measurements taken in all the test series are presented below depending on the  $H_s/H_p$  ratio (equal to 2.5, 2.0 or 1.5).

Figure 4 shows the relationship between the applied average total impact energy and the total average drive of the poulder  $\sum S_{pi}$ . The total impact energy is calculated as the sum of the mass of the poulder multiplied by gravity and the height of the fall at each drop, divided by the area of the poulder's base. Despite the use of the same energy, the  $\sum S_{pi}$  decreases with the reduction of the thickness of the soft layer. All the relationships visible in Fig. 4 can be approximated with two linear segments (dashed lines) joined with a curve. Initially, the average drive of the poulder is independent of  $H_s/H_p$  ratio, but after about 3 drops, the current drive becomes the smaller the thinner is the soft layer, reaching eventually a constant value. It is worth noting that this stabilization occurs faster for smaller  $H_s$  value.

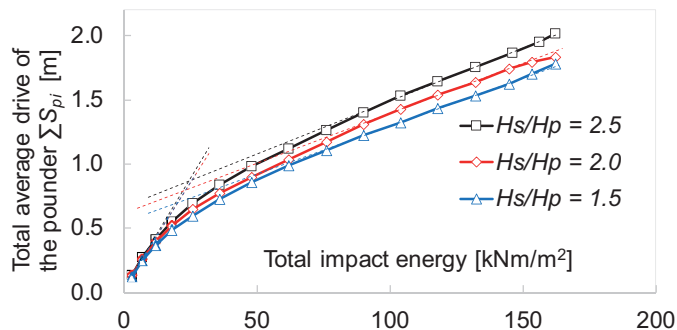


Fig. 4. The relationship between the total impact energy and the total average drive of the poulder

Since one of the most important parameters measured during formation of a DR column *in situ* is the current average drive of the poulder ( $S_p$ ), the observed vertical displacement of the column's base at its axis ( $S_c$ ) was compared with it and shown in Fig. 5. The obtained results are analysed below, together with the observed aggregate displacements for each  $H_s/H_p$  ratio.

Figure 6 presents the vectors of the resultant displacements of the backfill material in the column A ( $H_s/H_p = 2.5$ ) after the 1<sup>st</sup>, 5<sup>th</sup>, 8<sup>th</sup> and 14<sup>th</sup> drops of the poulder. Based on

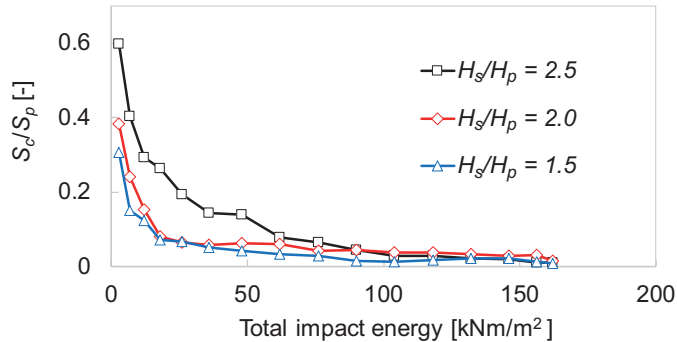


Fig. 5. The influence of the total impact energy on the  $S_c/S_p$  ratio – columns A, B, C

Fig. 5 and Fig. 6, the DR process can be divided into two stages. In the first one (1<sup>st</sup>–5<sup>th</sup> drops), the material was driven mainly downwards (in the vertical direction) (Fig. 6a–f) and the greatest displacement values occurred in the axis. The base of the column was semi-circular (Fig. 6a, c, d, f) or of a rounded wedge-shape (Fig. 6b, e). For the 1<sup>st</sup> drop of the poulder, the vertical displacement of the column base was equal to ca. 60% of the applied drive of the poulder, while at the 5<sup>th</sup> drop it was only 20% of  $S_p$ . In the outer parts of the columns, the aggregate moved also sideways, but during the first stage, the inclination of the displacement vectors  $\alpha$  (relatively the vertical axis) was very small: about 15–30° (Fig. 6a–f). In the second stage (6<sup>th</sup>–16<sup>th</sup> drops), the vertical displacements of the driven aggregate in the axis of the columns were clearly reduced: at the 6<sup>th</sup> and 7<sup>th</sup> drops the  $S_c/S_p$  ratios were equal to about 14% and decreased below 5% at the 10<sup>th</sup> drop (Fig. 5 and Fig. 6g–i). On the other hand, the inclinations of the resultant displacement vectors at the outer sides of the backfill material increased and  $\alpha$  reached 50° (Fig. 6j–l). The diameters<sup>1</sup> of the columns at the mid-height and in the lower parts increased. The semi-circular base, formed in the first stage (series 1 and 3), increased in size but kept this form until the column was finished (Fig. 6g, i, j, l). The shape of the base of the column in series 2 could also be described as semi-circular, with only a rounded wedge protruding at one side (Fig. 6h, k). In all the cases, where  $H_s/H_p = 2.5$ , the bases of the columns did not reach the load-bearing layer, so they can be called ‘floating’. It shall be noted that as the poulder hits the surface of the aggregate, its axis is rarely vertical, despite the undisturbed free fall. This has an impact on the trajectory of some part of the driven grains – it curves in the opposite direction (see e.g.: Fig. 6d, e). Nevertheless, eventually all the columns took the shape of a pear (Fig. 6j, k, l).

The vectors of the resultant displacements of the backfill material in the column B (0.4 m thick soft layer,  $H_s/H_p = 2.0$ ) after the 2<sup>nd</sup>, 5<sup>th</sup>, 9<sup>th</sup> and 14<sup>th</sup> drops of the poulder are shown in Fig. 7. In this behaviour, two stages can be distinguished as well. The first one, in which the largest vertical displacements of the base occurred in the column’s axis,

<sup>1</sup>The word ‘diameter’ is used here to refer to the *in situ* 3D cases, even though the conditions present in the model would rather suggest using the word ‘width’.



Fig. 6. The vectors of the resultant displacements of the backfill material – column A,  $H_s/H_p = 2.5$



Fig. 7. The vectors of the resultant displacements of the backfill material – column B,  $H_s/H_p = 2.0$

refers only to the first two drops – the  $S_c/S_p$  ratios were then equal to 38% and 24%, respectively (see Fig. 5). During the second stage, the increase of the depth in the axis of the column became much smaller and already at the 6th drop it fell below 5% of the current drive of the pounder (Fig. 5). The vertical displacements in the axis of the column were then accompanied by much larger vertical and horizontal displacements in the side zones. In the series 2 and 3, the inclination angles of the vectors ranged between 18 and 29° in the first stage (Fig. 7b, c) and, further, increased to even 64° (Fig. 7h, i, k, l). In the series 1, the inclination greater than 30° was reached after the 5th drop and the maximum  $\alpha$  was equal to 57° (Fig. 7g, j). The differences between series 1, 2, and 3 referred also to the shape of the columns' bases. In series 1, after the first three drops of the pounder (Fig. 7a), the base of the column was irregular in shape; after 4–6 drops it became semi-circular (Fig. 7d), and starting from the 7th one – practically flat (Fig. 7g, j). The column clearly reached the top of the sand layer after the 10th drop. The bases of the columns in series 2 and 3 were semi-circular from the beginning (Fig. 7b, c) and became flatter after about 5th drop (Fig. 7h, i). The final concave shape of the bases (Fig. 7k, l) results from the fact that the hydrogel (right behind the acrylic-glass wall) covered the gravel grains, which reached the bearing layer at the back of the testing box, making them undetectable for GOM. The greatest vertical displacements in the second stage were observed in the outer zones of the columns. Independently of the series, the final shape of the columns resembled a barrel with the largest diameter in the lowest part. As the gravel reached the sand layer, the columns can be called 'end-bearing'.

Figure 8 presents the vectors of the resultant displacements of MGr in the column C (0.3 m thick soft layer,  $H_s/H_p = 1.5$ ) after the 1st, 2nd, 6th and 14th drops of the pounder. The largest vertical displacement of the material driven into the hydrogel, occurred after the 1st drop of the pounder on the backfill material and amounted to only about 30% of  $S_p$ . The columns' bases were then semi-circular (Fig. 8a, b, c). During the successive pounder drops, the vertical grains' displacements in the axes of the columns decreased rapidly – for example: the  $S_c/S_p$  ratios after the 2nd and 3rd drop were equal to only 15% and 12%, respectively, and fell below 5% after the 6th drop. At the same time, the resultant displacements at the sides of the columns visibly increased and the columns' bases became flat (in series 1 and 3 – already after the 2nd drop of the pounder – see Fig. 8d,f) and remained so until the end of the test. The diameters of the columns in the lowest zones began to expand very quickly – the  $\alpha$  angles outside the axes of the columns were greater than 30° already after the first (series 2 and 3, Fig. 8b, c) or second (series 1, Fig. 8d) drop of the pounder. It shall be mentioned here that, contrary to the relatively symmetrical behaviour of the columns in series 1 and 3, the horizontal displacements of the grains in series 2 were asymmetrical – i.e. after the 1st drop of the pounder the  $\alpha$  angles on the left and right sides of the column were equal to 59° and 29°, respectively (Fig. 8b). This difference, however, was reduced in the further steps of the DR procedure, during which the angles in the lower parts of the columns increased greatly – up to: 70° in series 1, 80° in series 2 and 90° in series 3 (Fig. 8j, k, l). At the end of the test, the columns had the shape of a truncated cone with the largest diameter at the base (Fig. 8j, k, l). The main factor responsible for this shape, was reaching the load-bearing medium sand layer already after about 6 drops ('end-bearing columns'). It shall be noted that in the



Fig. 8. The vectors of the resultant displacements of the backfill material – column C,  $H_s/H_p = 1.5$

series 2, some part of the aggregate on the left side of the column was located further from the glass pane and hard to detect by the GOM program, thus the displacement vectors were shown for less number of grains (Fig. 8e, h, k). However, taking this fact into account, it may be assumed that the final shape of the column in series 2 is similar to the others.

## 6. Discussion and conclusions

The outcomes of the tests proved that the relative thickness of the soft layer ( $H_s/H_p$ ) largely affects the paths along which the grains in the backfill material are driven, resulting with columns of various final shapes and diameters.

A common feature in the most cases (7 out of 9) was the formation of the semi-circular column base in the first stage of the execution. It resulted from the largest vertical displacements under the axis of the pounder and additional horizontal movements in the side zones.

The further displacements of the driven backfill material depended on the distance between the base of the initial crater and the top of the load-bearing layer ( $\Delta$ ). In all the analysed cases, the first crater was approx. 0.2 m deep, so the initial distances were equal to 0.3 m, 0.2 m and 0.1 m for columns A, B and C, respectively. In relation to the width of the pounder ( $D_p$ ) it amounted to:  $3D_p$ ,  $2D_p$  and  $D_p$ .

When the DR was executed in the soft layer of the largest thickness (column A,  $H_s/H_p = 2.5$ ), the semi-circular base, formed in the first stage, was becoming wider and moved downwards, but kept the same shape. The distance  $\Delta = 3D_p$  was large enough for the backfill material to be pushed further down. The bearing layer had no influence on the process of replacement. As the material in the side zones moved at the angle  $\alpha \leq 50^\circ$ , the diameter was gradually increasing, giving eventually the shape of a pear (Fig. 6j, k, l).

In the column B ( $H_s/H_p = 2.0$ ), along with the decrease in the thickness of the soft layer, the influence of the load-bearing soil, present below, becomes visible. Not only the total average drive of the pounder gets smaller (Fig. 4), but also the effectiveness of the pounder to sink the backfill material underneath ( $S_c/S_p$ ) decreases much faster than in column A (Fig. 5). On the other hand, the material in the side zones has greater freedom of vertical movement, which results in flattening of the column's base. Additionally, the inclination of the displacement vectors increases from  $50^\circ$  (in column A) to  $64^\circ$  (in column B), resulting in lowering the relative depth at which the greatest diameter occurs. The side zones of the base of the columns stay rounded. The final shape of the column resembles an asymmetrical barrel (Fig. 7j, k, l).

When the distance  $\Delta$  is the smallest (column C,  $H_s/H_p = 1.5$ ), the influence of the bearing layer is becoming even more obvious. The differences observed between column B and A, are here accelerated: the reduction of the displacements between the top and bottom of the column in its axis is by almost 75% larger than in column A, while the  $\alpha$  angle in the side zones reaches even  $90^\circ$ . This results in forming the columns with the largest diameter and the shape of a truncated cone (Fig. 8j, k, l).

A certain analogy can be found between the analysed cases and the simple Boussinesq's solution for elastic homogenous half-space integrated for circular loading, where the zone affected by the loading, in the form of a 'pressure bulb', is limited to about twice the width of a footing [19]. Based on the observations presented above, it may be concluded that the depth affected by the process of the DR columns formation is equal to about three diameters of the poulder. If within this zone a harder layer is located – its presence causes flattening of the column's base and increase of its diameter.

The shapes of the columns obtained in the laboratory tests correspond well to the ones recorded in field (Fig. 1) for very similar  $H_s/H_p$  ratios and published in the literature. This fact allows us to assume that the displacements paths of the backfill grains in the real conditions will be similar to those observed in this study.

It is worth emphasizing that the differences in the behaviour recorded for the same types of columns at the same stage of the test, but executed in other series, resulted apparently from the natural variability of the backfill grading and from some minor differences in the procedure, like slightly other initial densities of the hydrogel or other angle at which the poulder touched the backfill surface. They were impossible to avoid, just like it is impossible in the field conditions. Nevertheless, the average patterns of the observed behaviour seem to be independent of these factors.

## Funding

This work was supported by the Polish National Centre for Research and Development (Narodowe Centrum Badań i Rozwoju), "Solidarity with scientists" programme [grant No.: SzN/I/33/DRPRO/2022, Experimental analysis of the formation process of dynamic replacement columns under laboratory conditions].

## References

- [1] B. Hamidi, "Distinguished ground improvement projects by dynamic compaction or dynamic replacement", PhD thesis, Curtin University, Australia, 2014. [Online]. Available: <http://hdl.handle.net/20.500.11937/66>.
- [2] M. Łupieżowiec and P. Kanty, "Analysis of dynamic replacement column construction process on neighbouring engineering structures", *Archives of Civil Engineering*, vol. 61, no. 3, pp. 3–18, 2015.
- [3] P. Stinnette, M. Gunaratne, G. Mullins, and S. Thilakasiri, "A quality control programme for performance evaluation of dynamic replacement of organic soil deposits", *Geotechnical and Geological Engineering*, no. 15, pp. 283–302, 1997, doi: [10.1023/A:1018467810200](https://doi.org/10.1023/A:1018467810200).
- [4] Ch. Chua, M. Lai, G. Hoffmann, and B. Hawkins, "Ground improvement using dynamic replacement for NCIG Cet3 Coal Stockyard", *Australian Geomechanics*, vol. 43, no. 3, pp. 63–74, 2008.
- [5] S. Kwiecień, *Odsztatcalność kolumn wymiany dynamicznej ustalana na podstawie próbnych obciążeń*. Gliwice, Poland: SUT Press, 2019.
- [6] S. Kumar, "Reducing liquefaction potential using dynamic compaction and construction of stone columns", *Geotechnical and Geological Engineering*, no. 19, pp. 169–182, 2001, doi: [10.1023/A:1016672106067](https://doi.org/10.1023/A:1016672106067).
- [7] P. Wong and M. Lacazedieu, "Dynamic replacement ground improvement – field performance versus design prediction for the Alexandria City Centre Project", in *Proceedings of a three day conference on advances in geotechnical engineering, organised by the Institution of Civil Engineers and held at the Royal Geographical Society: Advances in geotechnical engineering: The Skempton conference, London, UK, on 29–31 March 2004*. London: Thomas Telford Publishing, 2004, pp. 1193–1204.

- [8] S. Kwiecień, "Influence of load plates diameters, shapes of columns and columns spacing on results of load plate tests of columns formed by dynamic replacement", *Sensors*, vol. 21, no. 14, art. no. 4868, 2021, doi: [10.3390/s21144868](https://doi.org/10.3390/s21144868).
- [9] S. Kwiecień and M. Kowalska, "Dynamic replacement: the influence of poulder diameter and ground conditions on shape and diameter of the columns", *Architecture Civil Engineering Environment*, vol. 16, no. 1, pp. 71–84, 2023, doi: [10.2478/acee-2023-0005](https://doi.org/10.2478/acee-2023-0005).
- [10] Y. Oladosu, M.Y. Rafii, F. Arolu, S.C. Chukwu, M.A. Salisu, I.K. Fagbohun, T.K. Muftaudeen, S. Swaray, and B.S. Haliru, "Superabsorbent polymer hydrogels for sustainable agriculture: a review", *Horticulturae*, vol. 8, no. 7, art. no. 605, 2022, doi: [10.3390/horticulturae8070605](https://doi.org/10.3390/horticulturae8070605).
- [11] S. Kwiecień, Ed. *Kolumny kamienne formowane w technologii wymiany dynamicznej*. Gliwice, Poland: SUT Press, 2012.
- [12] R. Jasiński, K. Stebel, and J. Domin, "Application of the DIC technique to remote control of the hydraulic load system", *Remote Sensing*, vol. 12, no. 21, art. no. 3667, 2020, doi: [10.3390/rs12213667](https://doi.org/10.3390/rs12213667).
- [13] PN-EN ISO 17892-4:2017-01 Geotechnical investigation and testing – Laboratory testing of soil – Part 4: Determination of particle size distribution. PKN, 2017.
- [14] PN-88/B-04481 Grunty budowlane. Badania próbek gruntu. PKNMiJ, 1988.
- [15] PN-EN ISO 17892-3:2016-03 Geotechnical investigation and testing – Laboratory testing of soil – Part 3: Determination of particle density. PKN, 2016.
- [16] PN-EN ISO 17892-10:2019-01. Geotechnical investigation and testing – Laboratory testing of soil – Part 10: Direct shear tests. PKN, 2019.
- [17] PN-EN ISO 17892-5:2017-06. Geotechnical investigation and testing – Laboratory testing of soil – Part 5: Incremental loading oedometer test. PKN, 2017.
- [18] S. Pisarczyk, "Wytrzymałość gruboklastycznych gruntów z dorzecza Górnej Wisły stosowanych w nasypach budowli hydrotechnicznych", *Prace Naukowe Politechniki Warszawskiej. Inżynieria Środowiska*, vol. 32, pp. 5–51, 2000.
- [19] J.A.R. Ortigao, *Soil Mechanics in the Light of Critical State Theories. An introduction*. Balkema, 1995.

## **Badania laboratoryjne wpływu miąższości warstwy słabej na trajektorie przemieszczeń materiału zasypowego w kolumnach formowanych metodą wymiany dynamicznej**

**Słowa kluczowe:** geotechnika, kolumna kamienna, metoda wymiany dynamicznej, trajektorie przemieszczeń, warstwa słaba, wzmacnianie podłoża gruntowego

### **Streszczenie:**

Wymiana dynamiczna jest jedną z metod wzmacniania słabego podłoża stosowaną na świecie od blisko 50 lat, polegającą na formowaniu w podłożu kolumn z materiału gruboziarnistego i/lub bardzo gruboziarnistego. Kolumny wykonuje się ubijakami o masach od 5 do 20 ton, zrzucającymi z wysokości 15–25 m. W pierwszej kolejności, na skutek zrzutu ubijaka, w słabym podłożu powstaje krater, do którego wsypany jest materiał okruszony o frakcjach od piaszczystej, przez żwirową aż do, najczęściej, kamiennej. Jest on poddawany kolejnym zrzutom ubijaka i następującym po nim zasypom. Materiał ten zostaje wtłoczony w podłoże. W trakcie tego procesu, oprócz przemieszczeń pionowych, dochodzi do przemieszczania się ziaren w poziomie. Przeprowadzone przez jednego z autorów inwentaryzacje kolumn w warunkach *in situ* wykazały wpływ warunków gruntowodnych, w tym w szczególności miąższości słabego gruntu, na kształty końcowe kolumn. Skłoniło to autorów do podjęcia badań laboratoryjnych dotyczących procesu przemieszczania się kruszywa

w trakcie jego wbijania w warstwie słabej o różnej miąższości ( $H_s$ ) równej 1,5, 2,0 i 2,5 krotności wysokości stosowanego ubijaka ( $H_p$ ).

Podstawą badań była budowa stanowiska umożliwiającego obserwację procesu formowania kolumn oraz zastosowanie materiału symulującego warstwę słabą charakteryzującego się przezroczystością. Pierwsze wymaganie spełniała prostopadłościenna skrzynia o zewnętrznych wymiarach 1,5 m (szerokość)  $\times$  1,0 m (wysokość)  $\times$  0,15 m (grubość) wyposażona od czoła w szkło akrylowe. Wymaganie drugie uzyskano przez zastosowanie usieciowanego polimeru akrylowego mieszanego z wodą destylowaną w stosunku 1:15 (wagowo) w wyniku czego uzyskiwano miękkoplastyczny żel. Kolumny były wykonywane ze żwiru średniego, a warstwę nośną symulował piasek średni. Wymiary ubijaka, uziarnienie kruszywa stosowanego na kolumny oraz miąższości słabego gruntu dobrano stosując skalę geometryczną 1:10 w stosunku do warunków rzeczywistych. Badania wykonano w trzech seriach, dla trzech różnych miąższości podłoża. Łącznie uformowano 9 kolumn wymiany dynamicznej.

Proces formowania kolumn był rejestrowany z zastosowaniem kamery o częstotliwości nagrywania 50 kl/s. Analizę przemieszczeń kruszywa w miękkoplastycznej mieszance przeprowadzono w programie GOM. Dla poszczególnych etapów formowania kolumn wyznaczono wektory przemieszczeń wbijanego materiału oraz ustalono kształty końcowe kolumn.

Przeprowadzone badania wykazały, że miąższość słabej warstwy ma wpływ na sposób przemieszczenia się kruszywa kolumn wymiany dynamicznej w trakcie ich formowania, co z kolei skutkuje wykonaniem kolumn o różnych kształtach i różnych podstawach. Cechą wspólną jest uformowanie w pierwszym etapie półkolistej podstawy kolumn. Jest ona wynikiem występowania największych przemieszczeń pionowych w osi formowania oraz przemieszczania się materiału bocznych stref kolumny również w kierunku poziomym. Dalsze przemieszczenia wbijanego materiału kolumn zależą od odległości między podstawą zasypanego krateru a stropem warstwy nośnej.

W przypadku wbijania materiału w warstwę słabą o największej miąższości ( $H_s/H_p = 2,5$ ), uformowana w pierwszym etapie, półkolistą podstawą, w wyniku dalszego formowania, zaczyna się poszerzać i przemieszczać pionowo w dół, zachowując swoją formę do końca procesu wbijania. Warstwa nośna nie ma wpływu na kształt podstaw kolumn i proces ich formowania. Ponieważ materiał w bocznych strefach kolumn przemieszcza się pod kątem do  $50^\circ$  od pionu ich średnica rośnie wraz z głębokością, co w połączeniu z półkolistą podstawą nadaje kolumnom kształt „gruszki”.

Wraz ze zmniejszeniem miąższości słabej warstwy ( $H_s/H_p = 2,0$ ) obserwowany jest wpływ warstwy nośnej na przemieszczenia materiału kolumn. Zmniejszają się wpędy pionowe materiału w osi podstawy formowanej kolumny, z kolei materiał z bocznych stref ma większą swobodę przemieszczeń w pionie przez co podstawa kolumn spłaszcza się i rozszerza na boki (wektory przemieszczeń nachylone pod kątem do  $64^\circ$ ). Ponieważ boczne strefy podstawy kolumn są zaokrąglone uzyskują one kształt niesymetrycznej „beczki” z największą średnicą w dolnej części kolumny.

W przypadku formowania kolumn w warstwie o najmniejszej miąższości ( $H_s/H_p = 1,5$ ) wpływ warstwy nośnej jest największy. Przemieszczenia pionowe wbijanego materiału w osi kolumny zmniejszają się, z kolei te w bocznych strefach formowanych kolumn zwiększają, co powoduje spłaszczenie podstawy. Ze względu na równoczesne zwiększenie kątów rozchodzenia się materiału w strefach bocznych do nawet  $70\text{--}90^\circ$  kolumny mogą bardzo szybko osiągać duże średnice w podstawie. Uformowane kolumny mają płaskie podstawy i kształt odwróconego ściętego stożka.

Uzyskane w badaniach laboratoryjnych kształty kolumn są zbliżone do kolumn uzyskiwanych w warunkach polowych przy podobnym stosunku miąższości warstwy wzmacnianej do wysokości ubijaka. Można na tej podstawie wnioskować, że zaobserwowane w niniejszej pracy trajektorie przemieszczeń dobrze odzwierciedlają zachowanie materiału zasypowego w warunkach rzeczywistych.